Variation of the Thickness and Number of Wells in the CdS/HgS/CdS Quantum Dot Quantum Well System†

Markus Braun, Clemens Burda, and Mostafa A. El-Sayed*

School of Chemistry and Biochemistry, Georgia Institute of Technology, Atlanta, GA, 30332-0400

Received: January 3, 2001; In Final Form: May 1, 2001

We report on the first chemically prepared multilayer quantum well structure in a semiconductor quantum dot. By subsequent precipitation of HgS, CdS, HgS, and again CdS from aqueous solution, we obtained nanoparticles which contain two HgS quantum wells separated by a double layer of CdS. The core and the capping material is also CdS. The two-well system was characterized by absorption and emission spectroscopy, which clearly reveal the formation of a two-well and not a single double-layered quantum well system. This system allows to study the interaction of quantum wells that are separated by different thicknesses of the CdS barriers. The radiative and relaxation dynamics of the new two-well system are compared with the dynamics of systems having a single-layer well and a double-layer well system.

Introduction

In recent years, an increasing interest in semiconductor quantum well structures has led to the formation of physically and chemically prepared quantum well systems.[1−7] Multiple-layered quantum wells are meanwhile used to build solid-state optoelectronic devices.[8−10] The first chemically prepared quantum well system was synthesized in the CdS quantum dot.[1,2] Since its preparation, this quantum dot quantum well (QDQW) system has attracted much attention, both experimentally[11−16] and theoretically.[17−19]

The pioneering work of Mews et al. led to a variety of QDQWs. These nanoparticles consist of a tetrahedral CdS core with 111 facets. By adding Hg^{2+} ions to the colloidal CdS solution, the outermost shell of CdS is exchanged for HgS, the much more insoluble chemical. This leads to an HgS monolayer. This HgS well layer is capped with additional CdS, leading to a stable quantum well heterostructure. The thickness of the core, well, and the clad can be varied during the course of the synthesis.

Quantum wells having multiple layers are prepared by expensive physical methods, which require clean-room and UHV conditions. A chemical synthesis of multiple quantum wells in nanoparticle units could provide a low-cost pathway of preparation. Moreover, convenient handling of the quantum well units by wet-chemical modification and deposition from the solution at ambient conditions promises new applications. A theoretical study by Chang and Xia[19] reported on a two-layer QDQW system, but the realization of a multiple layered QDQW system is still lacking.

In this paper we report on the first preparation of a two-layered QDQW system. The results of the optical spectroscopy are compared to the single-layer well[11,12] and the double-layer well[13] system.

Experimental Section

The experimental setup of the fs-time-resolved transient absorption experiment is described in detail elsewhere.[13] The sample solution was optically excited with pulses at 400 nm (duration of 100 fs (fwhm), pulse energy of 100 μJ). The electron−hole dynamics in the colloidal solution was probed by a white light continuum pulse (450 nm to 1050 nm), which was generated by focusing a small part of the fundamental laser output at 800 nm into a sapphire plate. The white light pulse and the excitation pulse were focused and overlapped in the colloidal sample, and the change of the sample absorption due to the excitation pulse was probed with the white light pulse as a function of the delay time between the two pulses. The delay time was varied by an optical delay line with a resolution of 3 μm (21 fs). The colloidal solution in a 2-mm thick glass cell was rotated to prevent photodegeneration of the sample.

The photoluminescence spectra of the colloidal solution were recorded in a 90° setup. The samples were excited at 440 nm by an OPO, which was pumped by the third harmonic of a Q-switched Nd:YAG laser (pulse duration 5 ns at 10 Hz). The photoluminescence of the sample was recorded by a system of cutoff filter, monochromator, and CCD camera. The photoluminescence spectra were corrected for the Raman bands and background by subtracting a spectrum with water as reference sample. All experiments were performed with the sample at room temperature.

Sample Preparation. The synthesis route of the presented QDQW nanoparticles can be separated in three main steps: (A) growing of the CdS core, (B) exchanging the outermost CdS monolayer by HgS, and (C) growing a CdS monolayer on the nanoparticle. The details of these preparation steps are reported elsewhere.[2,13] Here the principles of the preparation and the order of the steps (A), (B), and (C) are summarized below.

In step A, CdS nanoparticles are prepared under argon atmosphere by injecting 0.6 mL H_2S gas into a 250 mL flask containing 100 mL 2×10^{-4} M aqueous solution of Cd^{2+} ions and hexametaphosphate as stabilizer while stirring at an initial pH of 7.9. The high pH value leads to a fast ionization of the H_2S gas into H^+ and S^- ions and thereby initiates a fast nucleation process of many small CdS crystallites. As S^- precipitates CdS, an increase in the dissociation of H_2S leads to an increase of the H^+ concentration, which lowers the pH value to an acidic range after about 30 s. Thereby, a slow

† Part of the special issue "Edward W. Schlag Festschrift".
* Corresponding author.

10.1021/jp010002l CCC: $20.00
Published on Web 05/22/2001

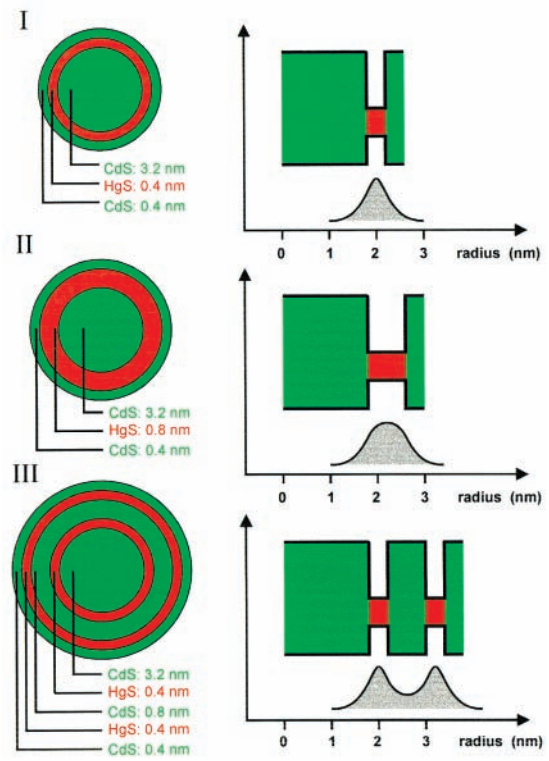

Figure 1. Schematic structure of the prepared QDQW systems having different thickness and number of wells (in red color), for the actual dimensions see text. The actual shape of small CdS crystallites was shown to be tetrahedral. On the right of the QDQW structures the wave functions for the charge carriers are sketched as calculated in Figure 4 of ref 18.

growing of the CdS crystallites can occur until a size of 3.5 nm is reached. The final pH value is reached at 4.6. Subsequently, the colloidal solution is purged with argon for 20 min to remove the excess H_2S.

In step B, by adding 12 mL aqueous solution of 10^{-3} M Hg^{2+} ions at a pH of 7.0 to the colloidal solution, the Cd^{2+} ions of the surface layer of the nanoparticles is exchanged by the Hg^{2+} ions. This is because the solubility product of HgS is 26 orders of magnitude smaller than that for CdS. Thereby one monolayer of CdS is replaced by one monolayer of HgS. The exchanged Cd^{2+} ions remain in the solution. The number of these free Cd^{2+} ions is sufficient to form one monolayer of CdS, if S^- ions would be provided.

In step C, to grow one monolayer of CdS on the nanoparticles, the appropriate amount of Cd^{2+} ions has to be present in the colloidal solution. This is automatically the case if step B was performed immediately before this step, otherwise the correct amount of Cd^{2+} has to be injected through a septum into the flask. Then a CdS monolayer is grown on the nanoparticles by slowly injecting H_2S/water solution dropwise over a 25 min period at a pH of 7.0. After that, the colloidal solution is purged for at least 20 min with argon to remove the excess H_2S. By applying these three steps in various order, the following QDQW systems I, II, and III were prepared. A sketch of these systems is shown in Figure 1.

Single-Layer Well QDQW: System I, $CdS/(HgS)_1/(CdS)_1$. This system consists of a CdS core, which is surrounded by one monolayer of HgS and capped by one monolayer of CdS (see Figure 1). The order of steps for the synthesis route here is simply step A−B−C. During step A, the CdS core is grown, then with step B the HgS well layer is formed, and finally with step C the HgS well layer is capped with a monolayer of CdS.

Double-Layer Well QDQW. System II, $CdS/(HgS)_2/(CdS)_1$. This system consists of a CdS core, which is surrounded by one double-layer of HgS and capped by one monolayer of CdS (see Figure 1). The synthesis is performed in the order step A−B−C−B−C. With the initial three synthesis steps, system I is prepared. From this point we exchange the monolayer of CdS with HgS by applying step B. Then, with step C, the final monolayer of CdS is grown on the nanoparticle.

Two-Wells QDQW. System III, $CdS/(HgS)_1/(CdS)_2/(HgS)_1/(CdS)_1$. This system consists of a CdS core, one monolayer of HgS, two monolayers of CdS, a second monolayer of HgS, and a final CdS monolayer as capping (see Figure 1). The synthesis is performed in the order step A−B−C−C−C−B−C. Again, the initial three synthesis steps lead to system I. From there, by applying step C twice, three monolayers of CdS are grown around the HgS monolayer. The third CdS layer is then exchanged for an HgS monolayer using step B, and with the final step C this HgS monolayer is capped by a monolayer of CdS. This leads to the structure where two independent HgS well layers are formed in a CdS nanoparticle, separated by two monolayers of CdS.

All systems have a 3.2 nm CdS core and a single-layer CdS capping of 0.4 nm thickness. In system I, a single-layer HgS quantum well of 0.4 nm thickness is placed between core and clad. For system II, the well layer was extended to a double-layer HgS quantum well of 0.8 nm thickness. In system III, the two HgS single layer quantum wells, each of 0.4 nm thickness, are separated by a CdS double-layer of 0.8 nm thickness.

Results and Discussion

Absorption Spectra. In Figure 2, the absorption spectra of the prepared QDQW systems at room temperature are shown. The spectra were taken after each synthetic step starting with the CdS core. The spectra show a continuous red-shift of the absorption edge, which is due to the increase of either the HgS well or the nanoparticle size in each step. The order of the shown spectra for QDQW system I with increasing red-shift is (a) CdS, (b) $CdS/(HgS)_1$, and (c) $CdS/(HgS)_1/(CdS)_1$. For the QDQW system II, the order of the absorption spectra taken is (a) CdS, (b) $CdS/(HgS)_1$, (c) $CdS/(HgS)_1/(CdS)_1$, (d) $CdS/(HgS)_2$, and (e) $CdS/(HgS)_2/CdS$. The absorption spectra for the QDQW system III are shown also with increasing red-shift in the series of nanoparticles (a) CdS, (b) $CdS/(HgS)_1$, (c) $CdS/(HgS)_1/(CdS)_1$, (d) $CdS/(HgS)_1/(CdS)_3$, (e) $CdS/(HgS)_1/(CdS)_2/(HgS)_1$, and (f) $CdS/(HgS)_1/(CdS)_2/(HgS)_1/(CdS)_1$.

By comparing the absorption edges of the three systems, one notices that for system III with two separated quantum wells, it is red-shifted compared to the single-well QDQW system I, but still higher in energy compared to that for the double-well QDQW system II. The minima of the second derivative of the absorption for the different QDQW systems are at 625 nm for system I, 700 nm for system II, and 670 nm for system III, giving the lowest energy of the optically allowed transitions for each system.

Also, the oscillator strength for the lowest exciton absorption of the QDQW system III is comparatively greater than that for systems I and II, which can be understood by the fact that one nanoparticle of system III contains approximately the double amount of atoms as that of system I. On the other hand, the amount of HgS equals that in system II, but an oscillator strength twice as large is measured for the two-layer system. Therefore, we assume that it is the mixing of the states from the two HgS quantum wells that leads to the newly allowed transitions at 670 nm.

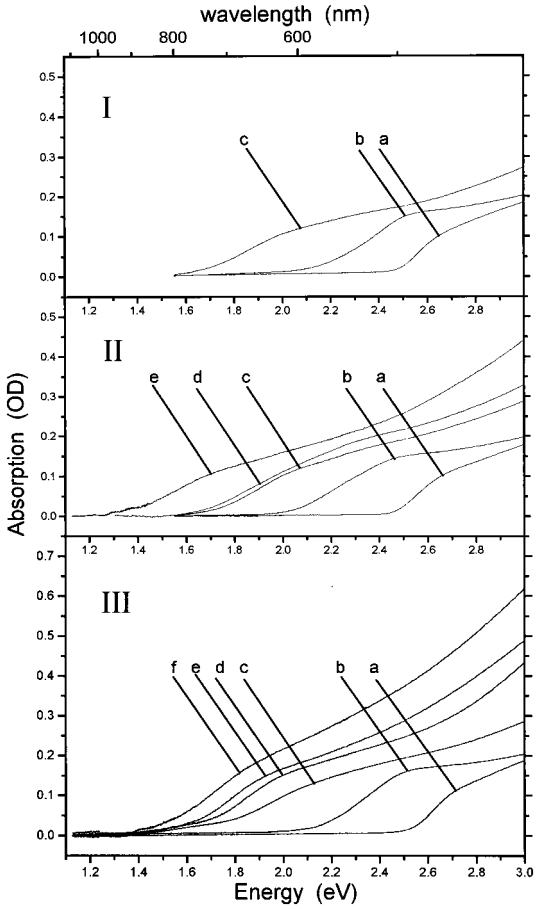

Figure 2. Absorption spectra of the three QDQW systems. The spectra of each system are presented as obtained after each synthesis step. Beginning with the CdS core spectrum at 470 nm, each synthesis step leads to a red shift of the nanoparticle absorption as described in the text. For system I, three spectra are shown for the CdS core (a), the $CdS/(HgS)_1$ core−shell (b), and the $CdS/(HgS)_1/(CdS)_1$ QDQW system (c), which shows the lowest allowed transition at 625 nm. For system II, five spectra are shown. The first three spectra are identical to system I (a, b, c). The spectrum (d) resembles the absorption of the $CdS/(HgS)_1/(HgS)_1$ core−shell and the most red-shifted spectrum (e) represents the transitions of the double-layer QDQW with the lowest transition at 700 nm and same oscillator strength as system I. For system III, six spectra are shown with the first three spectra being identical to system I (a, b, c). The following spectra show the transitions of $CdS/(HgS)_1/(CdS)_3$ (d), $CdS/(HgS)_1/(CdS)_2/HgS$ (e), and the two-well QDQW (f) at 670 nm. Interestingly, the oscillator strength of the two-well QDQW is enhanced by a factor of 2 compared to the other two systems.

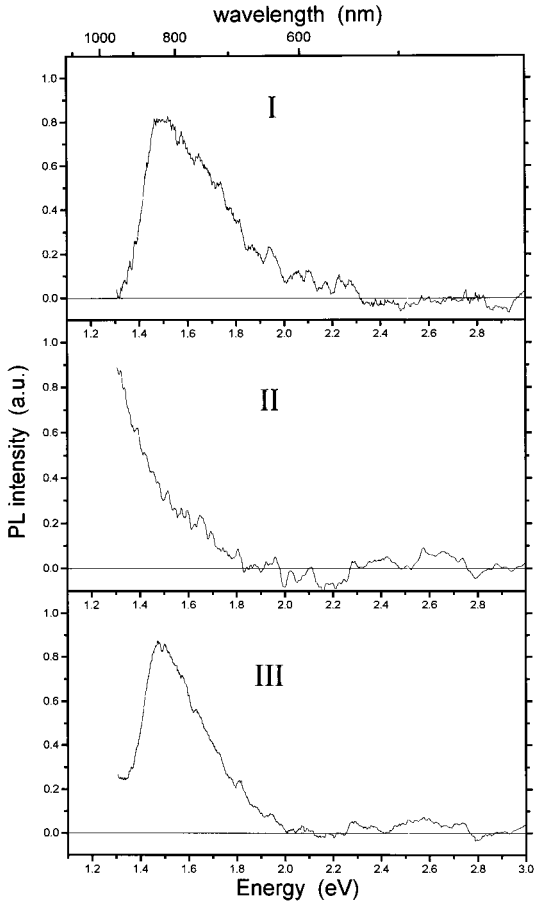

Figure 3. Emission spectra of the QDQW systems I, II, and III. The emission maximum for system I is at 820 nm, and for system II at 950 nm. For system III the emission appears at 820 nm, the same wavelength as for the single-layer QDQW system I. The onsets of the emission spectra show the same trend as the absorption spectra in Figure 2, namely that the energy of lowest transition of III is between the energies of system I and II, indicating that the additional HgS in III does not increase the initial HgS layer thickness but a second separated HgS well is formed.

Emission Spectra. The photoluminescence spectra of the three QDQW systems are shown in Figure 3. The photoluminescence is very weak for all systems (the quantum yield is estimated to be lower than 1%), and the broad emission is mainly due to emission from trap states most likely located at the CdS/HgS interface or the surface of the nanoparticles. The onset of the photoluminescence for systems I, II, and III shifts in a manner similar to their absorption edge, so that the emission onset for system III lies energetically between that for system I and system II. However, the maxima of the photoluminescence show another behavior. For the QDQW system I and III, this maximum is found to be at 820 nm, but for system II it is more strongly red-shifted to 950 nm. This indicates that the predominant trapping state is identical for systems I and III, which both have HgS monolayers for their quantum wells, whereas that state is red-shifted for system II, which has a HgS double-layer as well. This indicates that the trap state, which is the origin of this emission, is determined by the HgS well thickness and is therefore not located at the particle surface. This leads to the conclusion that the observed trapping site can be found at the CdS/HgS interface. That interface was observed and discussed before as the origin of lattice imperfections in a TEM study[3] of the QDQW system I and in the ODMR study,[15] in which the structure of these trapping sites was studied by ESR using their photoluminescence.

Energy Dependence of the Relaxation Dynamics. The dependence of the observed decay time of these systems after excitation at 400 nm is studied as a function of energy within the absorption and emission spectral regions and is shown and compared in Figure 4. For each system, a similar behavior is observed. In the high-energy part of the negative transient absorption signal, a short-lived component with a lifetime of about 5 ps is observed, whereas in the low-energy part, a distribution of decay times can be found with the decay time increasing with increasing wavelength. The wavelengths at which the long-lived component appears first are 600, 700, and 650 nm for systems I, II, and III, respectively. These wavelengths can be correlated with the onset of the photoluminescence spectrum for each system.

A negative transient absorption signal can be due either to bleach or to stimulated emission of the sample, and a bleach signal can be observed only in a spectral range where the sample absorbs. Therefore, the long-lived component of the three

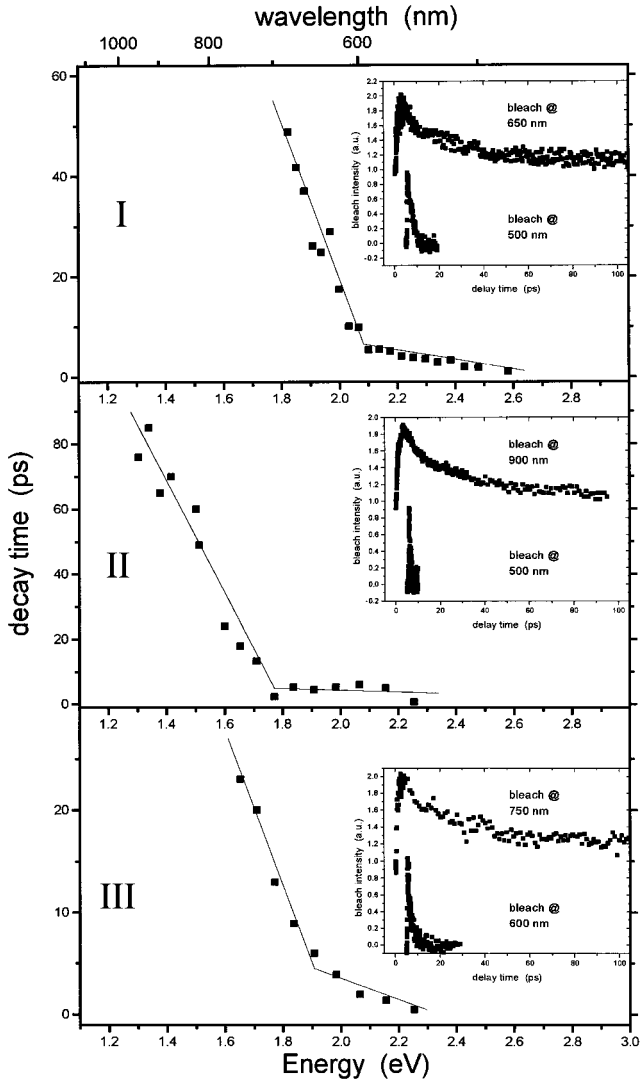

Figure 4. Decay times of the negative transient absorption signals as a function of the observation wavelength upon excitation at 400 nm in all three systems (typical kinetic traces are shown as inset). Two wavelength regimes can be identified, namely long-lived and short-lived signals. In the absorption region the bleach recovery is found to have a short decay of ~5 ps. In the emission region the stimulated emission is found to have a long lifetime, which increases by increasing the wavelength. The transition for these two regimes are found at 600 nm for system I, 700 nm for system II, and 650 nm for system III, as indicated by the interception of the shown lines. The lines were fitted by a least-squares method but are rather intended as a visual aid. The trend of the interception wavelength is found to be consistent with the absorption and photoluminescence in Figures 2 and 3.

systems has to be attributed to a stimulated emission signal. This component is observed in the same spectral range as the photoluminescence for the three samples. The distribution of long-lived decay times can therefore be attributed to the stimulated emission of the carrier recombination in the trapping states within their inhomogeneous distribution.

The short-lived component in the higher energy range therefore has to be explained by the bleach of the low energy excitonic state, which has an optically allowed transition to the ground state.

The theoretical predictions by Jaskolski and Bryant[18] for systems I and II are in agreement with the experimental observations of the hole-burning results,[3,14] line-narrowing,[3,14] and transient absorption[11−14] spectroscopy. Unfortunately there are no theoretical calculations available for the energy of the lowest excitonic states of the QDQW system III, in which two wells of HgS monolayers are separated by two layers of CdS.

Conclusion

Three different QDQW systems were investigated with a single-layer, double-layer, and two single-layer HgS wells inside the CdS nanoparticle. The system with two wells has a double-layer of CdS separating them. The absorption, photoluminescence and transient absorption measurements show that the energy of the lowest excitonic state is shifted to the red, if a second HgS well layer is added to the QDQW system. That shift is smaller, if the second well layer is separated from the first one by a barrier of two CdS layers. But, nevertheless, the observation of a red shift indicates that the well layers are not independent of each other. Our future project is to investigate the strength and nature of the interaction between the charge carriers in the two wells as function of the thickness of the CdS barrier and the thickness of the HgS wells themselves.

Acknowledgment. This work was supported by the office of Naval Research (contract No. N00014-95-1-0306). M.B. also thanks the Alexander von Humboldt Foundation for financial support (Feodor Lynen Fellowship).

References and Notes

(1) Eychmüller, A.; Mews, A.; Weller, H. *Chem. Phys. Lett.* **1993**, *208*, 59.

(2) Mews, A.; Eychmüller, A.; Giersig, M.; Schooss, D.; Weller, H. *J. Phys. Chem.* **1994**, *98*, 934.

(3) Mews, A.; Kadavanich, A. V.; Banin, U.; Alivisatos, A. P. *Phys. Rev. B* **1996**, *53*, R13242.

(4) Mews, A.; Eychmüller, A. *Ber. Bunsen-Ges. Phys. Chem.* **1998**, *102*, 1343.

(5) Dumas, Ph.; Derycke, V.; Makarenko, I. V.; Houdre, R.; Guaino, P.; Downes, A.; Salvan, F. *Appl. Phys. Lett.* **2000**, *77*, 3992.

(6) Ahn, Y. H.; Yahng, J. S.; Sohn, J. Y.; Yee, K. J.; Hohng, S. C.; Woo, J. C.; Kim, D. S.; Meier, T.; Koch, S. W.; Lim, Y. S.; Kim, E. K. *Phys. Rev. Lett.* **1999**, *82*, 3879.

(7) Kim, D. S.; Ko, H. S.; Kim, Y. M.; Rhee, S. J.; Hohng, S. C.; Yee, Y. H.; Kim, W. S.; Woo, J. C.; Choi, H. J.; Ihm, J.; Woo, D. H.; Kang, K. N. *Phys. Rev. B* **1996**, *54*, 14580.

(8) Abeeluck, A. K.; Garmire, E.; Canoglu, E. *J. Appl. Phys.* **2000**, *88*, 5859.

(9) Shen, A.; Liu, H. C.; Gao, M.; Dupont, E.; Buchanan, M.; Ehret, J.; Brown, G. J.; Szmulowicz, F. *Appl. Phys. Lett.* **2000**, *77*, 2400.

(10) Kawakami, Y.; Narukawa, Y.; Omae, K.; Fujita, S.; Nakamura, S. *Appl. Phys. Lett.* **2000**, *77*, 2151.

(11) Kamalov, V. F.; Little, R.; Logunov, S. L.; El-Sayed, M. A. *J. Phys. Chem.* **1996**, *100*, 6381.

(12) Little, R. B.; Burda, C.; Link, S.; Logunov, S.; El-Sayed; M. A. *J. Phys. Chem. A* **1998**, *102*, 6581.

(13) Braun, M.; Burda, C.; El-Sayed, M. A., submitted.

(14) Yeh, A. T.; Cerullo, G.; Banin, U.; Mews, A.; Alivisatos, A. P.; Shank, C. V. *Phys. Rev. B.* **1999**, *59*, 4973.

(15) Lifshitz, E.; Porteanu, H.; Glozman, A.; Weller, H.; Pflughoefft, M.; Eychmüller, A. *J. Phys. Chem. B* **1999**, *103*, 6870.

(16) Koberling, F.; Mews, A.; Basché, T. *Phys. Rev. B* **1999**, *60*, 1921.

(17) Bryant, G. *Phys. Rev. B* **1995**, *52*, R16997.

(18) Jaskólski, W.; Bryant, G. *Phys. Rev. B* **1998**, *57*, R4237.

(19) Chang, K.; Xia, J.-B. *Phys. Rev. B* **1998**, *57*, 9780.